



**Get Clarity On Generics**

Cost-Effective CT & MRI Contrast Agents



FRESENIUS  
KABI

WATCH VIDEO

**AJNR**

**Neuromas and meningiomas: evaluation of early enhancement with dynamic MR imaging.**

K Fujii, N Fujita, N Hirabuki, T Hashimoto, T Miura and T Kozuka

*AJNR Am J Neuroradiol* 1992, 13 (4) 1215-1220

<http://www.ajnr.org/content/13/4/1215>

This information is current as  
of August 23, 2025.

# Neuromas and Meningiomas: Evaluation of Early Enhancement with Dynamic MR Imaging

Keiko Fujii,<sup>1</sup> Norihiko Fujita,<sup>1</sup> Norio Hirabuki,<sup>1</sup> Tsutomu Hashimoto,<sup>1</sup> Takashi Miura,<sup>1</sup> and Takahiro Kozuka<sup>1</sup>

**Purpose:** To investigate the role of dynamic MR imaging in the differentiation of neuromas and meningiomas. **Methods:** Eleven patients with neuromas and 15 patients with meningiomas underwent dynamic contrast-enhanced MR imaging using a short TE FLASH sequence and a bolus injection of Gd-DTPA. **Results:** There was no significant difference between these tumors in the signal-enhancement increment at the late phase, which corresponds to the signal-enhancement increment between pre- and postcontrast images in conventional spin-echo imaging. However, the signal enhancement at the vascular phase, ie, the phase where the first passage of Gd-DTPA was recognized both in the arteries and veins, was approximately four times as high in meningiomas as in neuromas. The difference was statistically significant. Furthermore, meningiomas had a wider range of early signal enhancement than did neuromas, reflecting the histologic varieties: two angioblastic meningiomas had the highest values, and three fibroblastic the lowest values comparable with those of neuromas, while meningiomas with other subtypes had intermediate values. **Conclusions:** The results of this study indicate that the evaluation of early enhancement with dynamic MR imaging is helpful in the differentiation of neuromas and meningiomas, and possibly in the crude prediction of pathologic subtypes of meningiomas.

**Index terms:** Neuroma; Meninges, neoplasms; Brain neoplasms, magnetic resonance

AJNR 13:1215-1220, Jul/Aug 1992

With the development of rapid magnetic resonance (MR) imaging techniques, dynamic studies using a bolus injection of Gd-DTPA have been applied clinically. However, only a limited number of dynamic MR studies have been performed for brain tumors (1-3). Using a short TE (4 msec) fast low-angle shot (FLASH) sequence rather than a long TE one for T2\* contrast (4), we previously performed dynamic contrast enhanced studies based on the usual T1 contrast and obtained time-versus-intensity curves (TICs) for a variety of brain tumors, and in particular, a characteristic pattern for neuromas (5): all four neuromas in our preliminary study showed a gradual enhancement pattern within the time interval. In the present study, we focused on neuroma and another representative extraaxial tumor, meningi-

oma, and investigated the role of dynamic MR imaging in the differentiation of these tumors.

## Subjects and Methods

From May 1990 to June 1991, 11 patients with neuromas and 15 patients with meningiomas, all surgically proved, were studied with dynamic MR imaging as well as conventional pre- and postcontrast spin-echo imaging. The neuromas originated from the acoustic nerve in seven cases, glossopharyngeal in two, and trigeminal in two. The histologic subtype of each meningioma was classified according to the widely accepted scheme (6): fibroblastic in three cases, transitional in five, meningotheliomatous in five, and angioblastic in two.

All patients were examined on a 1.5-T MR unit with a circularly polarized head coil. For the purposes of the dynamic study, we devised a spoiled gradient-echo pulse sequence with a short TE of 4 msec. To minimize the TE under the limited gradient performance, the combination of an off-center signal acquisition with a high sampling rate of 67 kHz and a short RF pulse of 1.28 msec was employed (7). Since the use of such a short TE significantly reduces T2\* dephasing effects, even in a two-dimensional mode, and improves T1 contrast (8), this sequence was considered suitable for the dynamic study based on T1 contrast. Presaturation pulses with the section-selection gradients

Received October 31, 1991; accepted and revision requested December 9; revision received February 13, 1991.

<sup>1</sup> Department of Radiology, Osaka University Medical School, 1-1-50, Fukushima-ku, Fukushima, Osaka 553, Japan. Address reprint requests to Keiko Fujii, MD.

AJNR 13:1215-1220, Jul/Aug 1992 0195-6108/92/1304-1215

© American Society of Neuroradiology



were applied to reduce pulsation artifacts from blood flow caused by flow-related enhancement effects.

Scan parameters were: TR/TE/flip angle/number of signals averaged (NSA) = 45 msec/4 msec/45°/1, section thickness = 8 mm, acquisition matrix = 192 × 256, and field of view = 21 cm. The acquisition time was 10 seconds per image. This sequence was repeated 16 times during the total dynamic imaging time of 340 seconds (Fig. 1). The first 10 images were acquired consecutively and the remaining six with intervals of 40 seconds. Immediately after the scanning of the first image, 0.1 mmol of Gd-DTPA per kg of body weight was administered intravenously over about 10 seconds. The bolus injection was well-tolerated with no adverse side effects.

For tumor and contralateral normal brain tissues (predominantly white matter), signal intensities (SIs) were evaluated using standard region-of-interest measurements. For the tumor with cystic components, care was taken to contain only solid portions of the tumor for the SI measurements. SIs were normalized to those of the precontrast normal brain tissues and TICs were obtained for each tumor. For the quantitative evaluation of the TICs obtained, we calculated the following SI increments:  $\Delta_1 = SI_n - SI_1$ , and  $\Delta_2 = SI_{16} - SI_1$ , where  $SI_1$  and  $SI_{16}$  were normalized signal intensities measured on the first precontrast image and the last image, respectively.  $SI_n$  was defined as a signal intensity on the n-th image that showed the first passage of contrast media both in the arteries and veins to be filled.

## Results

Using the short TE FLASH sequence with the above imaging parameters, images having the usual T1 contrast with almost no T2\* dephasing were obtained (Fig. 2). Since presaturation pulses with the section-selection gradients were employed, flow-related enhancement effects were reduced and brain vessels were depicted as having hypointensity on precontrast images as shown in Figure 2. This enabled us to identify the vascular phase, ie, filling of arteries and veins during the first passage of contrast media. The vascular phase was observed between the third

and fifth images, and predominantly (19/26 cases) on the fourth image.

While normal brain tissues showed almost no discernible signal changes during the dynamic examinations, the patterns of TICs for the extraaxial tumors were classified into the two basic types: gradual increase with no peak pattern (type 1) and steep increase and subsequent gradual decrease or flat pattern (type 2). All neuromas (11/11), originating from different cranial nerves, and three meningiomas (three/15) demonstrated the type 1 TIC (Fig. 3). The histologic subtype of the three meningiomas was fibroblastic. For the remaining 12 meningiomas (five transitional, five meningotheliomatous, and two angioblastic), the TICs corresponded to the type 2 pattern (Fig. 4).

The identification of the vascular phase allowed the quantitative evaluation of the early pattern of enhancement for both types of TICs with the common index of  $\Delta_1$  (Fig. 5). Meningiomas had significantly greater  $\Delta_1$  values ( $0.60 \pm 0.44$ ) than did neuromas ( $0.16 \pm 0.10$ ). This difference was statistically significant ( $P < .01$ , Wilcoxon rank sum test). Meningiomas had a wider range of  $\Delta_1$  values than did neuromas, reflecting the histologic varieties: two angioblastic meningiomas had the highest values, and three fibroblastic meningiomas the lowest values, while transitional and meningotheliomatous meningiomas had intermediate values.

The quantitative evaluation of the later pattern of enhancement was analyzed based on  $\Delta_2$  values. The mean  $\Delta_2$  values of neuromas and meningiomas were  $0.67 \pm 0.16$  and  $0.58 \pm 0.23$ , respectively. The difference in  $\Delta_2$  value was not statistically significant ( $P > .05$ ) (Fig. 6).

## Discussion

Previous studies using conventional spin-echo imaging have reported its usefulness for the differentiation of neuromas and meningiomas, which frequently originate in similar locations such as in the cerebellopontine angle and at the skull base. The differentiation between neuromas and meningiomas was provided neither by SI differences (9, 10) nor relaxation time measurements (11), but most reliably by the morphologic characteristics, such as extension along the course of cranial nerves for neuromas and linear enhancement along the dura emanating from the dural margin for meningiomas (12, 13).

With the use of conventional spin-echo imaging, Watabe et al (14) obtained measurements of

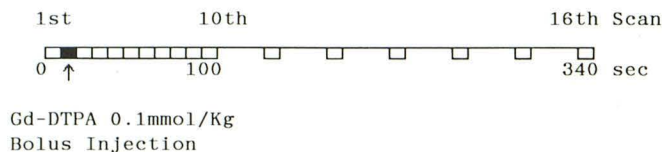


Fig. 1. Timing diagram of dynamic study. Sixteen images of single section were obtained during the total dynamic imaging time of 340 sec. The acquisition time per image was 10 sec. The first 10 images were acquired consecutively and the remaining six images with intervals of 40 sec. Immediately after the first scan, 0.1 mmol of Gd-DTPA per kg of body weight was administered over about 10 sec.



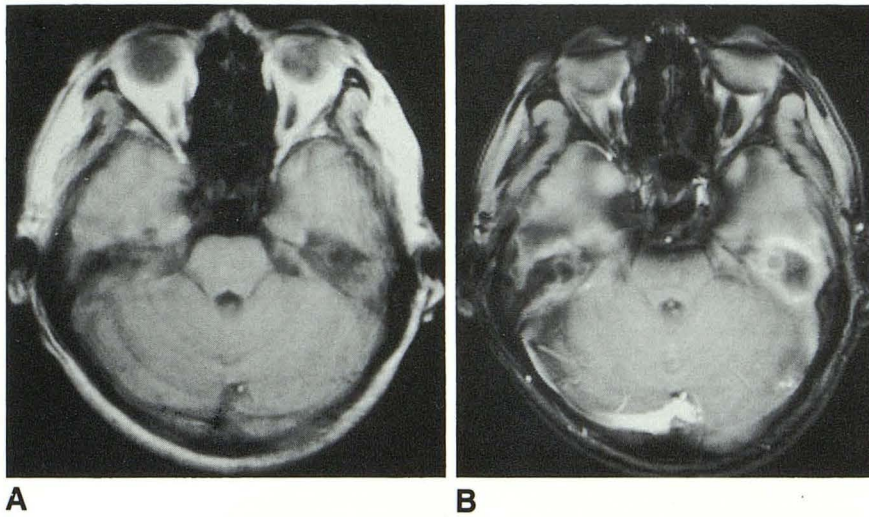


Fig. 2. Axial images of a normal volunteer at the level of the skull base using FLASH pulse sequences with different echo times: TE = 4 msec (A) and TE = 12 msec (B). Imaging parameters except for TE are the same: TR/flip angle/NSA = 45 msec/45°/4, section thickness = 8 mm, and acquisition matrix = 192 × 256. The short TE FLASH sequence provides improved T1 contrast with almost no T2\* dephasing compared to the longer TE one. Using this short TE FLASH sequence, dynamic study was performed.

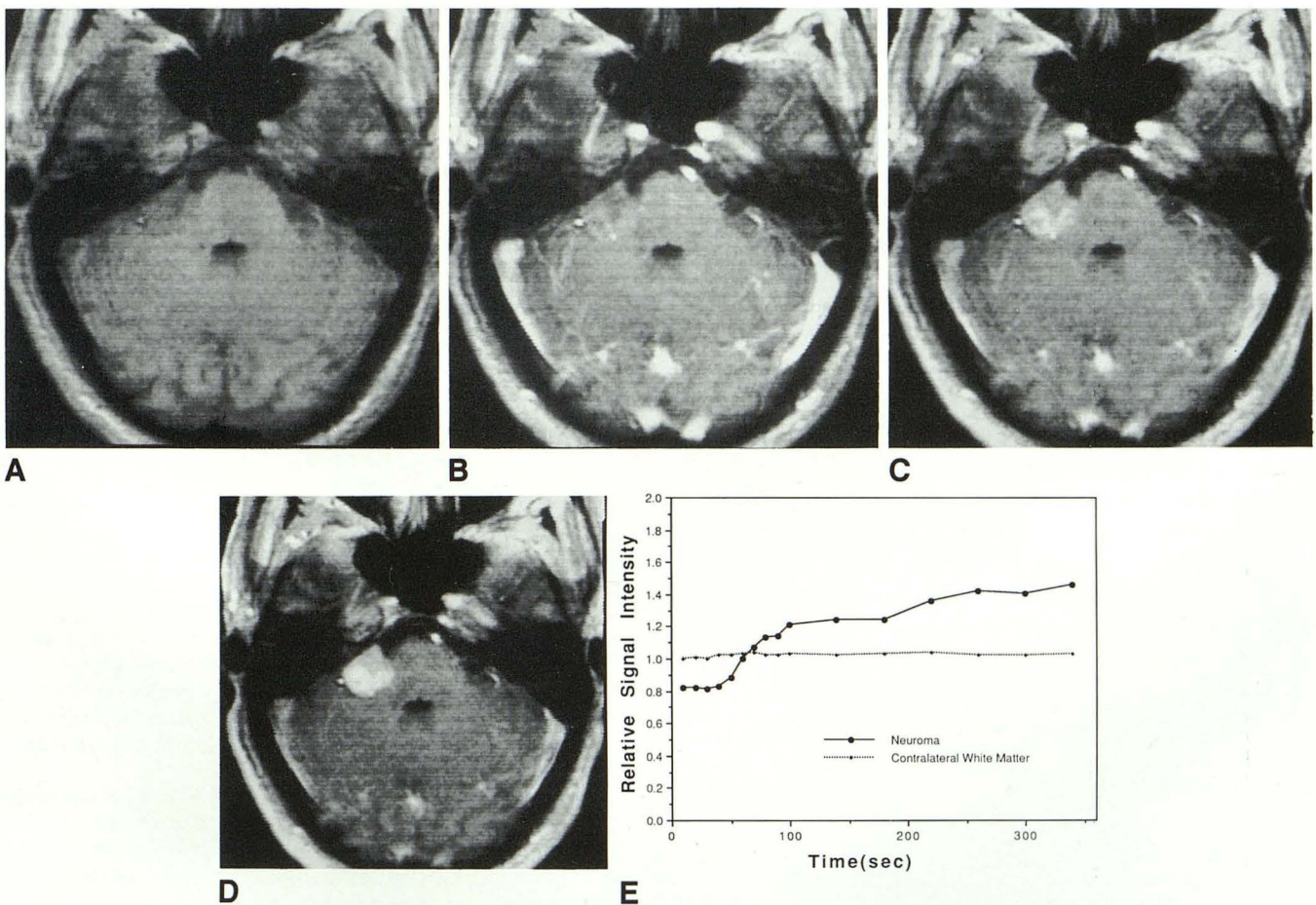


Fig. 3. Dynamic MR images (A-D) and time-intensity curve (E) of right acoustic neuroma. The short TE FLASH sequence was employed: TR/TE/flip angle/NSA = 45/4/45/1, 192 × 256 matrix and section thickness = 8 mm. Before (A) and 20 (B), 80 (C), 320 (D) sec after administration of Gd-DTPA. In the early image (B), the first passage of Gd-DTPA is seen in the arteries and veins. At this time, the tumor demonstrated only weak enhancement peripherally and entire enhancement with maximum signal intensity in the late image (D). The time-intensity curve of the tumor (E) corresponded to type 1, ie, gradual enhancement with no peak pattern. Normal contralateral white matter showed almost no discernible enhancement.



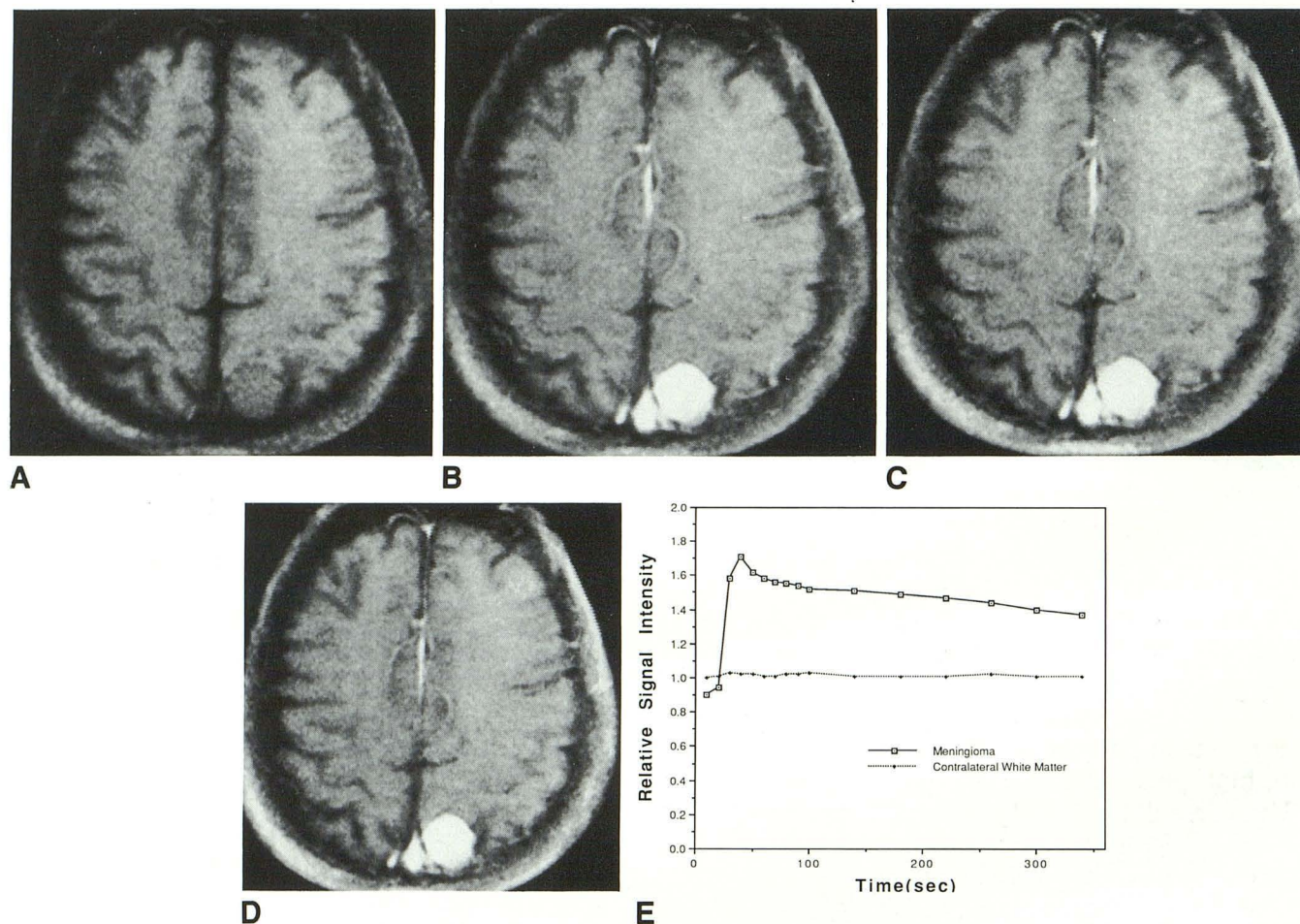


Fig. 4. Dynamic MR images (A–D) and time-intensity curve (E) of left parasagittal meningioma. The short TE FLASH sequence was employed: TR/TE/flip angle/NSA = 45/4/45/1,  $192 \times 256$  matrix, and section thickness = 8 mm. Before (A) and 20 (B), 80 (C), 320 (D) sec after administration of Gd-DTPA. The tumor was enhanced entirely with maximum signal intensity at the early phase (B), followed by gradual signal decrease in the later images (C and D). The time-intensity curve of the tumor corresponded to type 2, ie, steep increase and subsequent gradual decrease pattern.

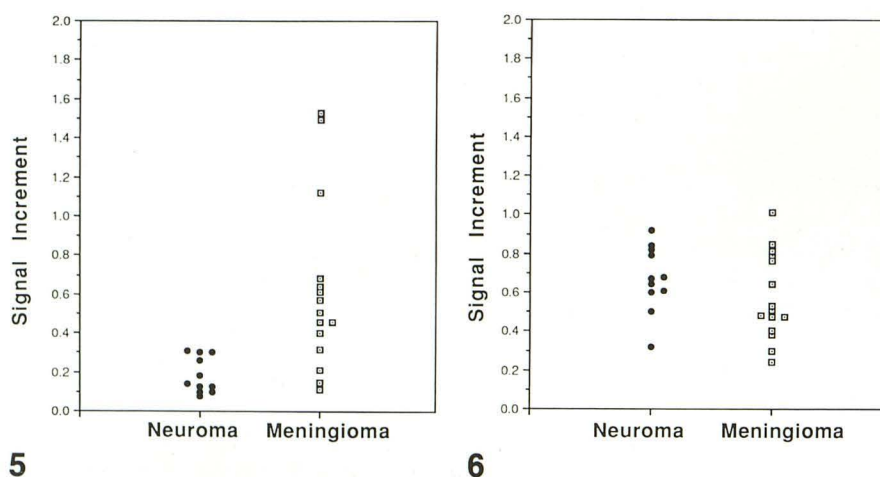


Fig. 5. Signal increments for neuromas and meningiomas at the vascular phase. Meningiomas had significantly greater early signal enhancement than did neuromas. Neuromas had consistently low signal enhancement, while meningiomas had a wider range, reflecting their histologic varieties: two angioblastic meningiomas had the highest values, three fibroblastic the lowest values, while meningiomas with other subtypes had intermediate values.

Fig. 6. Signal increments for neuromas and meningiomas at the late phase. The difference in the late enhancement was not statistically significant between neuromas and meningiomas.

signal enhancement and relaxation rate increments with Gd-DTPA for neuromas and meningiomas. They reported that the average T1 relax-

ation rate increment measured on pre- and post-contrast images was almost twice as high in neuromas as in meningiomas, mainly deriving



from longer intrinsic T1 values in neuromas. They also reported that the signal-enhancement increment was higher in neuromas than in meningiomas, but this difference was poorly appreciated on postcontrast images. In our dynamic studies, the  $\Delta_2$  value corresponds to the signal-enhancement increment in the later phase of stable distribution of Gd-DTPA, with this later period being the phase accessible to conventional MR. According to our data, the mean  $\Delta_2$  value of neuromas was also slightly higher than that of meningiomas, but the difference was not statistically significant.

In contrast to this, early transit data, as represented by the  $\Delta_1$  value, are not available with conventional MR. For the evaluation of the early patterns of enhancement in patients with brain tumors, dynamic CT studies have been conventionally used with bolus administration of iodinated contrast media. However, to our knowledge, only a few studies have described the early enhancement patterns for limited cases with neuromas and meningiomas (15–17): the former was manifested in most cases by slow wash-in and low plateau pattern and the latter by rapid wash-in, high peak, and subsequent decrease pattern. These results using dynamic CT are consistent with our dynamic MR results that all neuromas demonstrated type 1 TIC and meningiomas other than fibroblastic subtype demonstrated type 2 TIC.

The mechanism of enhancement with Gd-DTPA, similar to that with the iodinated contrast media (18), is complex but depends on the size of the intravascular compartment, represented by the tumor vascularity, as well as on the size of extravascular compartment and the actual permeability of the tumor vessels to the contrast agent. Theoretical approaches have been proposed to quantify these parameters using a multicompartimental model (19, 20), but they are complicated by the fact that the relationship between measured MR signal and tissue Gd-DTPA concentration is not given by a linear relationship.

For simplicity, we took a practical approach to the quantitative evaluation of the time course of enhancement by means of the signal increments,  $\Delta_1$  and  $\Delta_2$ . While the later enhancement in terms of  $\Delta_2$  mainly relates to the size of the extracellular space within the tumor, the initial rise of enhancement in terms of  $\Delta_1$  is considered to reflect, in part, the degree of the tumor vascularity. This is because the initial rise is proportional to the rate of leakage of the contrast medium from the

intravascular space, which is a function of the capillary surface area density and the permeability of the tumor vessels to the contrast media.

Our results based on the evaluation of early enhancement in terms of the  $\Delta_1$  value suggest that neuromas, wherever they originate, have slow initial rise, and hence, poor tumor vascularity, and that meningiomas usually have rapid initial rise, and hence, rich tumor vascularity. Although further investigation will be needed, a crude prediction of pathologic subtypes of meningioma may be possible on the basis of the degree of the early enhancement: tumors with low  $\Delta_1$  values comparable with those of neuromas tend to be fibroblastic, and tumors with relatively high  $\Delta_1$  values tend to be angioblastic.

In conclusion, dynamic MR imaging, in combination with bolus injection of Gd-DTPA, has enabled us to trace the time course of tumor enhancement in detail and may provide further information about CNS lesions, since the evaluation of early enhancement is helpful in the differentiation of neuromas and meningiomas.

## References

1. Koschorek F, Jensen HP, Terwey B. Dynamic MR imaging: a further possibility for characterizing CNS lesions. *AJNR* 1987;8:259–262
2. Vogl T, Bruening B, Schedel H, et al. Paragangliomas of the jugular bulb and carotid body: MR imaging with short sequences and Gd-DTPA enhancement. *AJNR* 1989;10:823–827
3. Bullock PR, Mansfield P, Gowland P, Worthington BS, Firth JL. Dynamic imaging of contrast enhancement in brain tumors. *Magn Reson Med* 1991;19:293–298
4. Edelman RR, Mattle HP, Atkinson DJ, et al. Cerebral blood flow: assessment with dynamic contrast-enhanced T<sub>2</sub>\*-weighted MR imaging at 1.5 T. *Radiology* 1990;176:211–220
5. Matsuoka H, Fujita N, Harada K, et al. *Dynamic contrast enhanced MR imaging of brain tumors: characteristic time-intensity curve for neuromas*. Presented at the Annual Meeting of the Society of Magnetic Resonance in Medicine, New York, August 1990
6. Russel DS, Rubinstein LJ. *Pathology of tumors of the nervous system*. 4th ed. Baltimore: William & Wilkins, 1977:48–73
7. Nishimura DG, Macovski A, Jackson JL, et al. Magnetic resonance angiography by selective inversion recovery using a compact gradient echo sequence. *Magn Reson Med* 1988;8:96–103
8. Haacke EM, Tkach JA, Parrish TB. Reduction of T<sub>2</sub>\* dephasing in gradient field-echo imaging. *Radiology* 1989;170:457–462
9. Mikhael MA, Ciric IS, Wolff AP. Differentiation of cerebellopontine angle neuromas and meningiomas with MR imaging. *J Comput Assist Tomogr* 1985;9:852–856
10. Press GA, Hesselink JR. MR imaging of cerebellopontine angle and internal auditory canal lesions at 1.5 T. *AJNR* 1988;8:241–251
11. Just M, Thelen M. Tissue characterization with T<sub>1</sub>, T<sub>2</sub>, and proton density values: results in 160 patients with brain tumors. *Radiology* 1988;169:779–785
12. Tokumaru A, Ouchi T, Eguchi T, et al. Prominent meningeal enhancement adjacent to meningioma on Gd-DTPA enhanced MR images: histopathologic correlation. *Radiology* 1990;175:431–433

13. Goldsher D, Litt AW, Pinto RS, Bannon KR, Kricheff II. Dural "tail" associated with meningiomas on Gd-DTPA enhanced MR images: characteristics, differential diagnostic value, and possible implications for treatment. *Radiology* 1990;176:447-450
14. Watabe T, Azuma T.  $T_1$  and  $T_2$  measurements of meningiomas and neuromas before and after Gd-DTPA. *AJNR* 1989;10:463-470
15. Heinz ER, Dubois P, Osborne D, et al. Dynamic computed tomography study of the brain. *J Comput Assist Tomogr* 1979;3:641-649
16. Som PM, Lanzieri CF, Sacher M, Lawson W, Biller HF. Extracranial tumor vascularity: determination by dynamic CT scanning. *Radiology* 1985;154:401-412
17. Michael AS, Mafee MF, Valvassori GE, Tan WS. Dynamic computed tomography of the head and neck: differential diagnostic value. *Radiology* 1985;154:413-419
18. Bydder GM, Kingsley DP, Brown J, Niendorf HP, Young IR. MR imaging of meningiomas including studies with and without Gd-DTPA. *J Comput Assist Tomogr* 1985;9:690-697
19. Tofts PS, Kermode AG. Measurement of the blood-brain barrier permeability and leakage space using dynamic MR imaging: fundamental concepts. *Magn Reson Med* 1991;17:357-367
20. Brix G, Semmler W, Port R, et al. Pharmacokinetic parameters in CNS Gd-DTPA enhanced MR imaging. *J Comput Assist Tomogr* 1991;15:621-628